



Highly stable gold nanoparticles in an aqueous solution without any stabilizer prepared by a solution plasma process evaluated through capillary zone electrophoresis

Toshio Takayanagi¹ · Koji Miyake² · Sohta Iwasaki³ · Daiki Uehara⁴ · Hitoshi Mizuguchi¹ · Hirotaka Okabe⁵ · Naoki Matsuda⁵

Received: 12 April 2022 / Accepted: 7 June 2022 / Published online: 5 July 2022
© The Author(s), under exclusive licence to The Japan Society for Analytical Chemistry 2022

Abstract

Gold nanoparticles (AuNP) were prepared by a solution plasma process in the presence of H₂O₂, and they were dispersed in an aqueous solution without any stabilizer generally used. The dispersion stability of the AuNP in an aqueous solution was evaluated by capillary zone electrophoresis (CZE). An anionic broad peak was detected with the AuNP by CZE based on its wide variations in size and net charge. The broad peak also suggests that the AuNP were well dispersed in an aqueous solution. The dispersion stability of AuNP was evaluated from the viewpoints of long-term dispersion, salt concentration, and organic co-solvent. The anionic broad peak attributed to the dispersed AuNP was successfully detected for at least 55 weeks from the preparation with less shot signals of the aggregates. The AuNP was also well dispersed in aqueous NaCl solutions with its concentrations up to 30 mmol L⁻¹, as well as with ethanol co-solvent up to 40%(v/v). The AuNP prepared by the solution plasma process was proved to be highly stable in an aqueous solution.

Keywords Gold nanoparticles · Stabilizer-free · Solution plasma process · Dispersion stability · Capillary zone electrophoresis

Introduction

Gold nanoparticles (AuNP) are promising substance for the labeling and the detection of biogenic substances [1, 2]. When AuNP are used as a sensing material for the target substance(s), it is essential for the AuNP to be dispersed in an aqueous solution. Therefore, AuNP are also the analysis target on physicochemical characterizations, and various stabilizers have been developed [3]. A simple approach for the dispersion evaluation is the measurement of the UV–vis absorption spectrum, if the AuNP solution shows the plasmonic absorption band at around 520 nm or not. While AuNP are generally prepared and stabilized with citric acid, the stabilization of AuNP has also been developed with nonionic fluorosurfactant of Zonyl FSN [4], mercaptoacetic acid [5], boron-rich anionic cobalt complex [6], or *ω*-sulfonylated alkylsulfanylaniline [7]. Polymer matrices were found to be effective for the stabilization of AuNP, including poly(ethylene glycol methyl ether) [8], quaternized cellulose [9], chitin nanofibrils [10], longan polysaccharide [11], and microbial exopolysaccharide levan [12]. Reversible aggregation/dissolution of AuNP was realized

✉ Toshio Takayanagi
toshio.takayanagi@tokushima-u.ac.jp

✉ Naoki Matsuda
naoki.matsuda@aist.go.jp

¹ Graduate School of Technology, Industrial and Social Sciences, Tokushima University, 2-1 Minamijyousanjima-cho, Tokushima 770-8506, Japan

² Graduate School of Sciences and Technology for Innovation, Tokushima University, 2-1 Minamijyousanjima-cho, Tokushima 770-8506, Japan

³ Graduate School of Advanced Technology and Science, Tokushima University, 2-1 Minamijyousanjima-cho, Tokushima 770-8506, Japan

⁴ Department of Science and Technology, Faculty of Science and Technology, Tokushima University, 2-1 Minamijyousanjima-cho, Tokushima 770-8506, Japan

⁵ Sensing System Research Center, National Institute of Advanced Industrial Science and Technology, 807-1 Shukumachi, Tosu, Saga 841-0052, Japan

by freeze-drying/dissociation with citrate/mercaptoacetic acid-coated AuNP [5] or by drying/dissociation with PEG-coated AuNP [8]. Southern African plant extracts [13], cinnamon phytochemicals [14], aqueous extract of *Foeniculum vulgare* seeds [15], *Prunus domestica* gum [16], and *Elaeis guineensis* (oil palm) kernel extract [17] were also utilized for the stabilization. The dispersion stability of AuNP has been examined in 10% NaCl, 0.5% cysteine or 0.5% bovine serum albumin solutions [13, 14].

Separation analyses including liquid chromatography and capillary zone electrophoresis (CZE) are alternative evaluation methods for the characterization and the dispersion evaluation of AuNP in an aqueous solution [18–21]. AuNP are generally anionic, and they are resolved by CZE based on the charge/mass ratio; the size resolution of AuNP has been made by CZE [22–25]. The size resolution was developed with sodium dodecyl sulfate [23] or poly(sodium 4-styrenesulfonate) [25]. Separation buffer with borax is useful for the dispersion of surfactant- or polymer-coated AuNP [26], and the peak shape in the electropherogram was reduced to the size distribution of AuNP by Taylor dispersion analysis [26, 27]. The CZE analysis has also been used for the stability evaluation. Dispersion of AuNP in an aqueous solution was verified through the baseline stability, when AuNP was added in the separation buffer as a label-free detection reagent for amino acid; stable baseline without any shot signal or baseline drift was obtained with a glycine–citrate buffer [28]. Critical nanoparticle concentration was defined as one of the aggregation parameters for AuNP through the peak area/peak broadening in capillary electrophoresis [29]. Surface-coating was made with citrate stabilized AuNP, and cationic, nonionic, and anionic AuNP were prepared [30]. The stability was examined by CZE, and α -dihydrolipoic acid-capped AuNP were found to be dispersed stably even after 20 days [30]. The dispersion stability was examined by CZE with several buffers [31, 32]. Multiple highly efficient peaks but not reproducible were detected at high concentrations of the separation buffer, and the aggregation of AuNP was suggested [31, 32]. On the other hand, the aggregation phenomena of AuNP have positively been utilized as colorimetric detections [33, 34]. A solution of AuNP was mixed to the post CE eluate flow as a sheath flow, and the eluted polycation aggregates the AuNP and a color change was induced to the AuNP [33]. The detection scheme was applied to the detection of heavy metal ions with 11-mercaptopentadecanoic acid and 6-mercapto-1-hexanol co-functionalized AuNP [34]. In this way, the aggregation of AuNP is very delicate issue, and the quality control of AuNP is of great interest [35].

Two of the present authors (N. M. and H. O.) have developed a synthesis method of AuNP by a solution plasma (SP) process in the presence of H_2O_2 [36–38]. The plasma discharge was made in an aqueous 5.0% H_2O_2 solution between

two Au electrodes. Since H_2O_2 decomposes in a short period, the dispersed AuNP exists in an aqueous solution without any stabilizer. The AuNP thus prepared was subjected to the surface-enhanced Raman scattering platform [37]. Another group also synthesized AuNP by a liquid-phase plasma process [39]; the discharge was made in an aqueous $HAuCl_4$ solution between two tungsten electrodes. The surface of the AuNP was modified by adding sugar or biopolymer, and cytotoxic activity was examined with the AuNP [39]. A prominent merit on AuNP preparation with Au discharge electrodes is that any coexisting substance is not present in the AuNP solution, since H_2O_2 is easily degradable.

In this study, dispersion stability of the AuNP prepared by the SP process was evaluated through CZE. A broad peak of anionic AuNP was detected by CZE with less shot signals of aggregates. The broad peak was continuously detected over at least 55 weeks storage, and the AuNP was found to be stably dispersed in an aqueous solution for a long period. The AuNP was also stable in a saline solution, as well as in water–ethanol media.

Materials and methods

Apparatus

All CZE experiments were performed by a 3D CE system (Agilent Technologies, Waldbronn, Germany) equipped with a photodiode array detector. A fused-silica capillary (GL Sciences, Tokyo, Japan) was set in a cassette cartridge, and the cartridge was installed in the CE system. Dimensions of the separation capillary were 75 μm i.d., 375 μm o.d., 48.5 cm in total length, and 40 cm in effective length from the injection end to the detection point. The capillary cartridge was thermostated at 25 °C by circulating constant temperature air. A ChemStation software (Ver. B04.02, Agilent Technologies) was used for the control of the CE system, the data acquisition, and the data analysis. The inner wall of the capillary was refreshed daily by flushing with 0.1 mol L^{-1} NaOH for 10 min followed with purified water for 10 min.

A Transmission Electron Microscope (TEM) JEM-2100F (JEOL, Tokyo, Japan) was used for taking TEM images of the AuNP. The applied voltage of the electron gun was 200 kV, and the image resolution was 0.23 nm as the particle size. A JASCO (Tokyo, Japan) V-630 spectrophotometer equipped with 1 cm path-length quartz cells was also used to measure the UV–vis spectra of the AuNP solution.

Chemicals

A pair of high-purity Au rods (20 cm long, 2 mm ϕ , 99.99%, Tanaka Kikinzoku Kogyo K.K., Tokyo, Japan) was used as

solution plasma discharging electrodes. Separation buffer components of 4-(2-hydroxyethyl)-1-piperazineethanesulfonic acid (HEPES) and *N*-cyclohexyl-2-aminoethanesulfonic acid (CHES) were from Dojindo Laboratories (Kumamoto, Japan). Hydrogen peroxide (30%, Kanto Chemical, Tokyo, Japan) and sodium naphthalene-1-sulfonate (Tokyo Chemical Industry, Tokyo, Japan) were used as received. Other reagents were of analytical grade. Super ultra-pure water (18 M Ω -cm) was used for the dilution of the H₂O₂ solution, as well as for the preparations of the solutions in CZE analyses.

AuNP solutions were prepared as previously reported [36–38]. A 50 mL Pyrex beaker was used as an SP processing reaction cell. Two Au electrodes were set with the angle of 30° to the perpendicular direction into the SP reaction cell and the gap between them were kept at 0.5 mm. An aqueous solution of 5.0% H₂O₂ was poured into the reaction cell. A high-voltage bipolar pulsed power supply (MPS-06K-01C, KURITA Seisakusho, Kyoto, Japan) was used as a power source. The applied bipolar voltage, the pulse width, and the frequency were 2.0 kV, 2.5 μ s, and 20 kHz, respectively. The energization period was set at 5 min. One batch of the AuNP solutions was concentrated about fivefold by evaporating the solvent water by vacuum at ambient temperature.

Procedure for the CZE measurements

Separation buffers used in CZE were prepared with 10 mmol L⁻¹ HEPES–NaOH (pH 7.2 or 7.4), or 10 mmol L⁻¹ CHES–NaOH (pH 9.0). An adequate amount of sodium chloride or ethanol was added in the AuNP solution or in the separation buffer, if necessary. After the separation capillary filled with and equilibrated with a separation buffer, the AuNP solution was injected into the capillary from its anodic end at 50 mbar for 3 or 10 s. After both ends of the capillary were dipped into the buffer vials, a DC voltage of 20 kV was applied to the capillary for the CZE. The AuNP was photometrically detected at 250 nm. Effective electrophoretic mobility of AuNP (μ_{eff}) was calculated as in ordinary manner using the migration time of electroosmotic flow and a migration time of the peak top of the AuNP.

Results and discussion

TEM characterization of the AuNP

The AuNP solution prepared by the SP process showed red-dish-purple color, and a spectrophotometric absorption band at around 530 nm was observed; AuNP was successfully synthesized as reported [36–38]. It took about 5–10 days to obtain stable UV–vis spectrum, because the AuNP are

surface active and microbubbles or ultra-fine bubbles have been generated from the residual H₂O₂ in the AuNP solution.

We have previously measured zeta potential of the AuNP prepared by the SP process, and it was between –36 and –51 mV [37]. The negative zeta potential suggests that the AuNP prepared by the SP process is anionic, and the AuNP would be dispersed by their electrostatic repulsion.

To characterize the size and shape of the AuNP, the AuNP were trapped on a copper grid and TEM images were taken. A typical TEM image is shown in Fig. 1A. It is noticed from Fig. 1A that the shape of the AuNP is in wide diversity with elliptical sphere shapes. A histogram of the particle size distribution is also shown in Fig. 1B. A maximum distribution can be read at 15–20 nm diameter, and the average diameter was 20 \pm 14 nm (mean \pm SD, *n* = 300). Although a few particles larger than 100 nm in size were observed, their percentage was less than 1%. The average diameter measured in this study was close to the result in our previous report, 14 nm [37]. The average aspect ratio of the AuNP was also examined in this study, and it was 0.78 \pm 0.10 (mean \pm SD, *n* = 100). Since TEM observation is done after the evaporation of the solvent, and therefore, TEM characterization is not suitable for the dispersion evaluation in an aqueous solution. Thus, we were directed to utilize CZE for the dispersion evaluation of the AuNP.

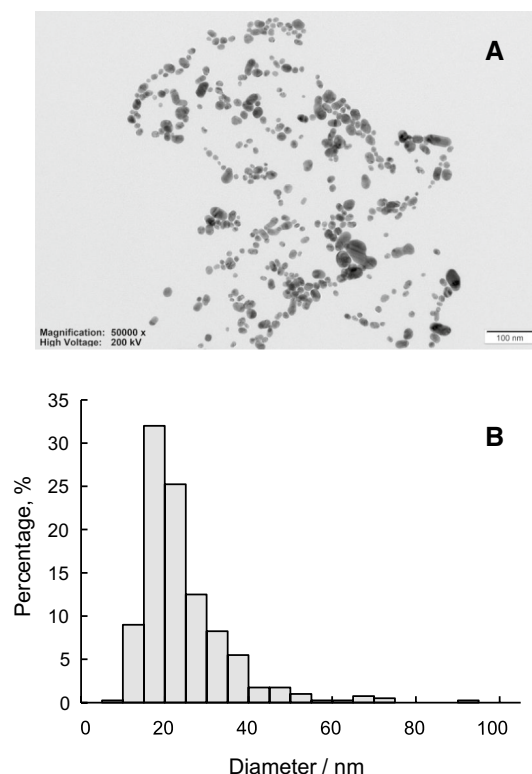


Fig. 1 **A** A TEM image of AuNP prepared by the SP process and **B** a histogram of the diameter of the AuNP (*n* = 300)

Long-term dispersion stability of the AuNP solution

Dispersion stability in an aqueous solution is one of the essential properties for AuNP to utilize them as labeling or detection reagents. As is discussed in the introduction section, various types of the surface modifier have been developed to suppress the aggregation of AuNP. Table 1 summarizes the stability evaluation of AuNP. UV–vis spectrophotometry is a popular tool to evaluate the dispersion status in an aqueous solution. CZE has also been used for the evaluation of the dispersion/aggregation of AuNP [22–27, 29–31], because CZE can directly handle the AuNP as its solution state.

CZE has been used for the detection and the characterization of AuNP, and broad peaks are often detected with positively or negatively charged AuNP [22–32]. CZE measurements were also examined in this study for the long-term dispersion study of the AuNP prepared by the SP process. Because hydrogen peroxide in the AuNP solution degraded and microbubbles/ultra-fine bubbles were generated just after the preparation of the AuNP solution, shot signals attributed to the bubbles were detected by CZE after 1 week of the preparation.

Typical electropherograms of the concentrated AuNP solution after ceasing the bubble generation are shown in Fig. 2. A broad peak attributed to the anionic AuNP was continuously detected for a long period at least up to 25 weeks from the

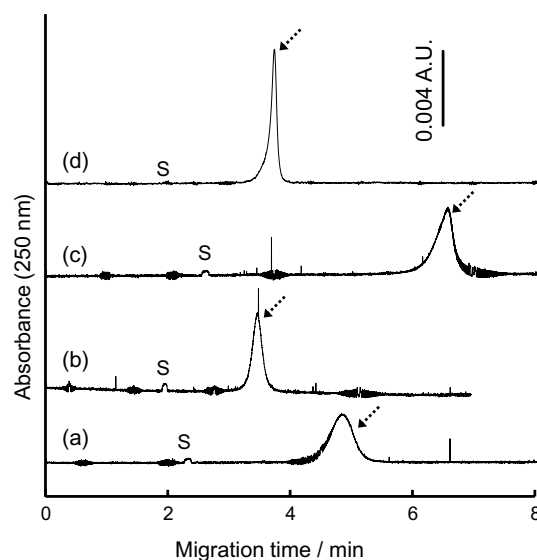


Fig. 2 Electropherograms of the concentrated AuNP solution stored for long-term periods. The anionic peak of AuNP is indicated with a dotted arrow. S: solvent (electroosmotic flow). Separation buffer: 10 mmol L⁻¹ HEPES–NaOH (pH 7.2). Storage period: (a) 3 weeks; (b) 11 weeks; (c) 17 weeks, (d) 25 weeks. CZE conditions: 20 kV applied voltage, 50 mbar×3 s sample injection, 25 °C capillary temperature, and 250 nm detection wavelength

Table 1 Stability evaluation of AuNP reported

Stabilizer	Evaluation method	Dispersion stability	Ref
Fluorosurfactant of Zonyl FSN	UV–vis	NaCl up to 500 mM	[4]
Mercaptoacetic acid	UV–vis	6 Freeze–thaw cycles	[5]
<i>ω</i> -Sulfonylated alkylsulfanylaniline	UV–vis	> 6 months	[7]
Poly(ethylene glycol methyl ether)	UV–vis	< 24 h ~ < 5 days	[8]
Quaternized cellulose	UV–vis	~ 4 months	[9]
Chitin nanofibrils	UV–vis	> 3 months	[10]
Longan polysaccharide	DLS, zeta potential	> 7 days at pH 4–10	[11]
Microbial exopolysaccharide levan	UV–vis	3–7 days	[12]
Southern African plant extracts	UV–vis	> 24 h in 10% NaCl, 0.5% cysteine or 0.5% BSA	[13]
Cinnamon phytochemicals	UV–vis	> 24 h in 10% NaCl, 0.5% cysteine or 0.5% BSA	[14]
Extract of <i>Foeniculum vulgare</i> seeds	UV–vis	> 24 h	[15]
<i>Prunus domestica</i> gum	UV–vis	> 6 months	[16]
<i>Elaeis guineensis</i> kernel extract / ionic liquid	UV–vis	> 120 days	[17]
Citrate	CZE	< 20 days	[30]
Pluronic F-127 (triblock copolymer)	CZE	< 20 days	[30]
Cetyltrimethylammonium	CZE	< 20 days	[30]
Dihydrolipoic acid	CZE	~ 20 days	[30]
(Unmodified)	CZE	Ammonium acetate < 20 mM	[31]
None	CZE	> 55 weeks ~ 30 mmol L ⁻¹ NaCl ~ 40%(v/v) ethanol	This study

preparation. It is also noticed that “shot signals” or “spike-like noises” are scarcely detected in the electropherograms over the period. AuNP are likely to aggregate to form precipitate, and therefore, stabilizers such as citrate are sometimes used to develop the dispersion. Electropherograms with less shot signals suggest that the AuNP are well dispersed in an aqueous solution as reported [28, 33], even though any stabilizer was not used in the SP process or under the storage conditions. It is reported that borate buffer is suitable for the detection of dispersed AuNP as a broad peak [26, 27, 30]. HEPES buffer is also found to be suitable for the detection of the dispersed AuNP. Increased ionic concentrations sometimes promote the aggregation of nanomaterial of graphene [40], and the low ionic concentration of the separation buffer would be helpful to detect the dispersed AuNP by CZE. The peak width of the AuNP is considerably wider than conventional CZE peaks. The shape of a broad peak corresponds to the wide variation of AuNP in its size and shape. Larger AuNP showed larger effective electrophoretic mobility [22, 23, 25], and the electrophoretic mobility is proportional to the radius of the particle [23]. A single CZE peak without shoulder also agrees with the result in size distribution of the AuNP: the distribution is one maximum at 15–20 nm. If plural diameter distributions were involved with the AuNP, corresponding plural peaks would have been detected by CZE [22, 23, 25].

Additionally, the anionic broad peak attributed to the AuNP was also detected with as-prepared AuNP solution over 55 weeks without serious shot signals, and the AuNP is well dispersed in an aqueous solution (Fig. S1). The peak area was smaller with the as-prepared AuNP, because of the low concentration of the as-prepared AuNP. The anionic broad peak was also detected with a different pH condition of 9.0 (CHES-NaOH). Long-term dispersion stability was also confirmed by UV–vis absorptiometry. A UV–vis spectrum after 8 weeks storage is shown in Fig. S2. Absorption maximum at 530 nm was still detected after the storage period. A considerable volume of AuNP solution is indispensable for every UV–vis spectrum measurement, which also directed us to utilize CZE for the monitoring of dispersion stability.

As can be seen in Fig. 2, the migration time of AuNP was not stable. CZE measurements have been done every week, and less stable velocity of EOF would be attributed to the difference in the migration time of AuNP. This particular instrument had also been used for different research, and hysteresis of electroosmotic flow was unavoidable, even though the capillary was refreshed daily. Therefore, the migration behavior of AuNP was evaluated with effective electrophoretic mobility, not with the migration time. Changes in the effective electrophoretic mobility of AuNP over the period is shown in Fig. 3 (open circle). Migration time of the peak top of the broad peak was used for the

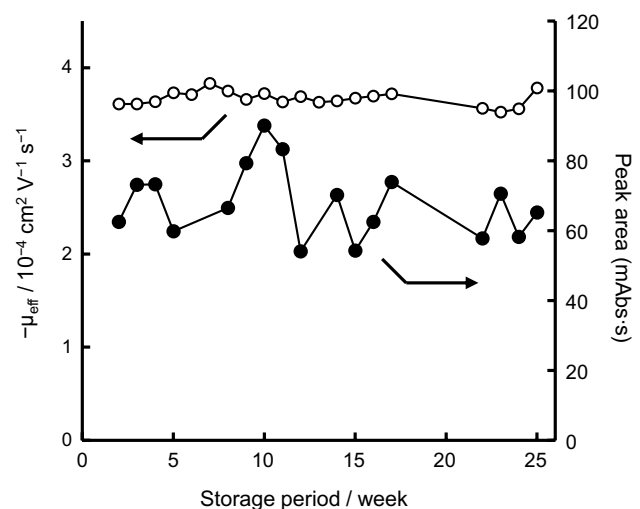


Fig. 3 Changes in effective electrophoretic mobility (open circle) and peak area (filled circle) of the AuNP with the storage period. Conditions are the same as in Fig. 2

calculation of the μ_{eff} value. While the migration time of AuNP was not stable, the effective electrophoretic mobility of AuNP was preferably stable at around $-3.7 \times 10^{-4} \text{ cm}^2 \text{ V}^{-1} \text{ s}^{-1}$ over the storage period. The result suggests that the AuNP is stably dispersed in an aqueous solution during the period and anionic charge of the AuNP changed little. The effective electrophoretic mobility of as-prepared AuNP was around $-3.5 \times 10^{-4} \text{ cm}^2 \text{ V}^{-1} \text{ s}^{-1}$, and the value is close to that of the concentrated AuNP. The close values of effective electrophoretic mobility suggest that the concentrated AuNP is still dispersed in an aqueous solution, in addition to the electropherograms of less shot signals.

Variation of the peak area for the AuNP over the storage period has also been examined; the result is also shown in Fig. 3 (filled circle). Although the peak area fluctuated, the fluctuation is attributed to the instable migration time of the AuNP. In CZE measurements, the peak area depends on the migration time of the peak, since the velocity of the analyte zone changes with the migration time. Less reproducibility of the injection volume in CZE would also be the reason for the fluctuation. Anyway, the peak area fluctuated in a range neither increasing or decreasing in this period, and the dispersed amount of AuNP changed little. The dispersion property of this AuNP is also summarized in Table 1.

Effect of salt concentrations on the dispersion stability of the AuNP

High concentrations of salt sometimes induce the aggregation of AuNP [4, 13, 14], and dispersion of AuNP is suppressed with higher concentrations of acetate buffer in the separation buffer yielding shot signals [31]. Dispersion

stability of the AuNP in the saline solution was examined in this study. An aliquot amount of NaCl was added in the concentrated AuNP solution, and the solution was stood for 24 h at room temperature. The incubated AuNP solutions were subjected to the CZE measurements. The results are shown in Fig. 4A. An anionic broad peak was successfully detected with the AuNP over the NaCl concentrations up to 30 mmol L⁻¹. However, the peak area decreased with increasing concentrations of NaCl. Some portion of the AuNP would have precipitated in the sample vial by the increased salt concentrations. The broad peak disappeared at 40 mmol L⁻¹ NaCl, and overlapped shot signals have been detected. The result suggests that the AuNP are partly aggregated and precipitated but still dispersed in an aqueous solution. Changes in the effective electrophoretic mobility of AuNP are shown in Fig. 4B. The value drastically decreased at 40 mmol L⁻¹ NaCl. It would be because of the decrease in charge/mass ratio by the formation of the aggregate. The aggregation/precipitation further proceeded at a higher concentration of 50 mmol L⁻¹ NaCl; even shot signals were not detected. The dispersion property of this AuNP with saline concentrations is also supplemented in Table 1.

Effect of an organic co-solvent on the dispersion stability of the AuNP

Since the AuNP are negatively charged, they are stabilized in an aqueous solution. Addition of organic co-solvent can reduce the dielectric constant of the solvent, and low

dielectric constant would promote the aggregation/precipitation of charged AuNP. Effect of ethanol addition on the dispersion of the AuNP was examined in this study. Separation buffers containing different percentages of ethanol were prepared, and aggregation of the AuNP in the separation capillary was investigated. Electropherograms with several ethanol percentages are shown in Fig. 5A. An anionic broad peak for AuNP was detected over the ethanol content up to 40% (v/v). The migration time of a broad peak got longer along with the increase in the ethanol content in the separation buffer. The result is also attributed to the reduced velocity of the EOF. The electrophoretic mobility depends on the viscosity of the separation buffer, and effective electrophoretic mobility of AuNP ($\mu_{\text{eff,AuNP}}$) was standardized with that of monoanionic naphthalene-1-sulfonate ion ($\mu_{\text{eff,1-NS}}$). The effective electrophoretic mobility of naphthalene-1-sulfonate ion was separately measured under identical separation buffers and CZE conditions. The result is shown in Fig. 5B. The standardized value declined a little with the ethanol percentage in the separation buffer. Decrease in the standardized effective electrophoretic mobility of AuNP suggests that the net surface charge of the AuNP would have reduced. Sodium ion in the separation buffer would have adsorbed on the AuNP through the improved electrostatic interaction in the water–ethanol solvent with its lower dielectric constant. Nevertheless, the AuNP is found to be stably dispersed in the ethanol–water solution, even though any stabilizer was not used with the AuNP. The dispersion property of this AuNP is also supplemented in Table 1.

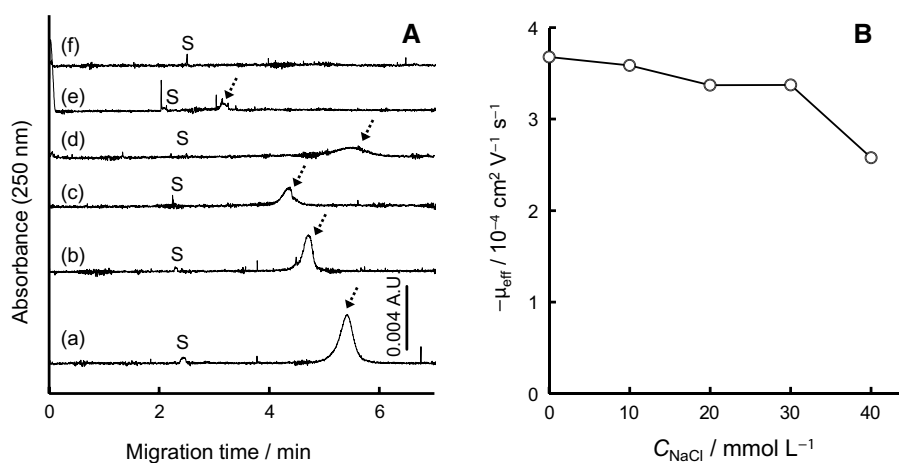


Fig. 4 **A** Electropherograms of the concentrated AuNP stored in saline solutions and **B** effective electrophoretic mobility of the AuNP. Separation buffer: 10 mmol L⁻¹ HEPES–NaOH (pH 7.2). Sample solution: concentrated AuNP solution + NaCl stood for 24 h. Concentrations of NaCl in the AuNP solution: (a), none; (b), 10 mmol L⁻¹;

(c), 20 mmol L⁻¹; (d), 30 mmol L⁻¹; (e), 40 mmol L⁻¹; (f), 50 mmol L⁻¹; CZE conditions: 20 kV applied voltage, 50 mbar × 3 s sample injection, 25 °C capillary temperature, and 250 nm detection wavelength

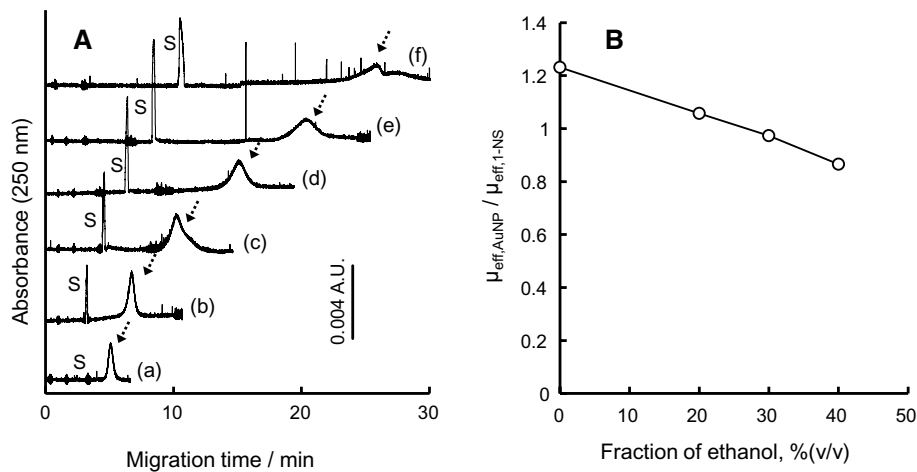


Fig. 5 **A** Electropherograms of the concentrated AuNP in the presence of ethanol in the separation buffer and **B** effective electrophoretic mobility of the AuNP standardized with that of naphthalene-1-sulfonate ion. Separation buffer: 10 mmol L⁻¹ HEPES–NaOH (pH 7.4) + ethanol. Ethanol content: (a), none; (b), 10%(v/v); (c),

20%(v/v); (d), 30%(v/v); (e), 40%(v/v); (f), 50%(v/v). Sample solution: concentrated AuNP solution. CZE conditions: 20 kV applied voltage, 50 mbar × 3 s sample injection, 25 °C capillary temperature, and 250 nm detection wavelength

Conclusions

Dispersion stability of the AuNP prepared by the SP process has been evaluated in an aqueous solution through the CZE analysis. An anionic broad peak was detected with the AuNP, and the AuNP is favorably dispersed in an aqueous solution with less aggregation/precipitation. The broad peak was continuously detected with the AuNP for a period of at least 55 weeks, as well as in aqueous NaCl solution up to 30 mmol L⁻¹ and in ethanol–water solution up to 40%(v/v) ethanol. It is revealed in this study that the AuNP prepared by the SP process is highly stable even though any stabilizer was not used.

Supplementary Information The online version contains supplementary material available at <https://doi.org/10.1007/s44211-022-00149-9>.

Acknowledgements The present authors acknowledge to Mr. Tomoyuki Ueki (a technical staff member of Tokushima University) for helpful assistance in the TEM observation.

Author contribution Toshio Takayanagi: Conceptualization, Methodology, Writing—Original Draft, Visualization, Supervision, Project administration, Funding acquisition. Koji Miyake: Validation, Formal analysis, Investigation, Data Curation, Visualization. Sohta Iwasaki: Validation, Formal analysis, Investigation. Daiki Uehara: Validation, Formal analysis, Investigation. Hitoshi Mizuguchi: Validation, Data Curation. Hirotaka Okabe: Resources, Investigation. Naoki Matsuda: Conceptualization, Resources, Writing—Review and Editing, Supervision.

Funding This work was partly supported by a Grant-in-Aid for Scientific Research (C) from the Japan Society for the Promotion of Sciences (JSPS) [grant number 20K05568].

Declarations

Conflict of interest The authors have no competing interests to declare that are relevant to the content of this article.

References

1. L. Qin, G. Zeng, C. Lai, D. Huang, P. Xu, C. Zhang, M. Cheng, X. Liu, S. Liu, B. Li, H. Yi, *Coord. Chem. Rev.* **359**, 1 (2018)
2. C. Kokkinos, *Nanomaterials* **9**, 1361 (2019)
3. J.W. Krumpfer, T. Schuster, M. Klapper, K. Müllen, *Nano Today* **8**, 417 (2013)
4. Q. Li, B. Lu, L. Zhang, C. Lu, *J. Mater. Chem.* **22**, 13564 (2012)
5. A.M. Alkilany, S.R. Abulateefeh, K.K. Mills, A.I. Bani Yaseen, M.A. Hamaly, H.S. Alkhatib, K.M. Aiedeh, J.W. Stone, *Langmuir* **30**, 13799 (2014)
6. K.R. Pulagam, K.B. Gona, V. Gómez-Vallejo, J. Meijer, C. Zilberfain, I. Estrela-Lopis, Z. Baz, U. Cossío, J. Llop, *Molecules* **24**, 3609 (2019)
7. M.I.M. Darwish, Y. Takenoshita, T. Hamada, S. Onitsuka, J. Kurawaki, H. Okamura, *J. Oleo Sci.* **66**, 1349 (2017)
8. H.H. Park, H. Park, A.C. Jamison, T.R. Lee, *Colloid Polym. Sci.* **292**, 411 (2014)
9. J. You, L. Zhao, G. Wang, H. Zhou, J. Zhou, L. Zhang, *J. Chromatogr. A* **1343**, 160 (2014)
10. Y. Huang, Y. Fang, L. Chen, A. Lu, L. Zhang, *Chem. Eng. J.* **315**, 573 (2017)
11. X. Zhang, L. Fan, Y. Cui, T. Cui, S. Chen, G. Ma, W. Hou, L. Wang, *NANO* **15**, 2050002 (2020)
12. O. Akturk, *Colloids Surf. B* **192**, 111061 (2020)
13. A.M. Elbagory, C.N. Cupido, M. Meyer, A.A. Hussein, *Molecules* **21**, 1498 (2016)
14. N. Chanda, R. Shukla, A. Zambre, S. Mekapothula, R.R. Kulkarni, K. Katti, K. Bhattacharyya, G.M. Fent, S.W. Casteel, E.J. Boote,

- J.A. Viator, A. Upendran, R. Kannan, K.V. Katti, *Pharm. Res.* **28**, 279 (2011)
15. M.K. Choudhary, J. Kataria, S. Sharma, *Appl. Nanosci.* **7**, 439 (2017)
16. N.U. Islam, R. Amin, M. Shahid, M. Amin, S. Zaib, J. Iqbal, *BMC Complement. Altern. M* **17**, 276 (2017)
17. M. Irfan, T. Ahmad, M. Moniruzzaman, S. Bhattacharjee, B. Abdullah, *Arab. J. Chem.* **13**, 75 (2020)
18. F.-K. Liu, *J. Chromatogr. A* **1216**, 9034 (2009)
19. U. Pyell, *Electrophoresis* **31**, 814 (2010)
20. C.-S. Wu, F.-K. Liu, F.-H. Ko, *Anal. Bioanal. Chem.* **399**, 103 (2011)
21. V. Adam, M. Vaculovicova, *Electrophoresis* **38**, 2389 (2017)
22. W.-M. Hwang, C.-Y. Lee, D.W. Boo, J.-G. Choi, *Bull. Korean Chem. Soc.* **24**, 684 (2003)
23. F.-K. Liu, Y.-Y. Lin, C.-H. Wu, *Anal. Chim. Acta* **528**, 249 (2005)
24. K.R. Riley, H. El Hadri, J. Tan, V.A. Hackley, W.A. MacCrehan, *J. Chromatogr. A* **1598**, 216 (2019)
25. R. Ciriello, P.T. Iallorenci, A. Laurita, A. Guerrieri, *Electrophoresis* **38**, 922 (2017)
26. U. Pyell, A.H. Jalil, C. Pfeiffer, B. Pelaz, W.J. Parak, *J. Colloid Interface Sci.* **450**, 288 (2015)
27. U. Pyell, A.H. Jalil, D.A. Urban, C. Pfeiffer, B. Pelaz, W.J. Parak, *J. Colloid Interface Sci.* **457**, 131 (2015)
28. F. Kitagawa, Y. Akimoto, K. Otsuka, *J. Chromatogr. A* **1216**, 2943 (2009)
29. M.R. Ivanov, H.R. Bednar, A.J. Haes, *ACS Nano* **3**, 386 (2009)
30. A. Pallotta, A. Boudier, P. Leroy, I. Clarot, *J. Chromatogr. A* **1461**, 179 (2016)
31. S. Dziomba, K. Ciura, P. Kocialkowska, A. Prah, B. Wielgomas, *J. Chromatogr. A* **1550**, 63 (2018)
32. S. Dziomba, K. Ciura, B. Correia, B. Wielgomas, *Anal. Chim. Acta* **1047**, 248 (2019)
33. T. Li, Z. Wu, W. Qin, *Anal. Chim. Acta* **995**, 114 (2017)
34. J. Bi, T. Li, H. Ren, R. Ling, Z. Wu, W. Qin, *J. Chromatogr. A* **1594**, 208 (2019)
35. A. Pallotta, A. Boudier, B. Creusot, E. Brun, C. Sicard-Roselli, R. Bazzi, S. Roux, I. Clarot, *Int. J. Pharm.* **569**, 118583 (2019)
36. N. Matsuda, T. Nakashima, *IEICE Tech. Rep.* **111**, 23 (2012)
37. N. Matsuda, T. Nakashima, H. Okabe, H. Yamada, H. Shiroishi, T. Nagamura, *Mol. Cryst. Liq. Cryst.* **653**, 137 (2017)
38. N. Matsuda, H. Okabe, T. Nagamura, M. Uehara, *Mol. Cryst. Liq. Cryst.* **686**, 63 (2019)
39. N. Treesukkasem, C. Chokradjaroen, S. Theeramunkong, N. Saito, A. Watthanaphanit, *ACS Appl. Nano Mater.* **2**, 8051 (2019)
40. M.B. Müller, J.P. Quirino, P.N. Nesterenko, P.R. Haddad, S. Gambhir, D. Li, G.G. Wallace, *J. Chromatogr. A* **1217**, 7593 (2010)